

## Effects of Sintering Temperature on Microstructural Properties of $\text{Ni}_{1-x}\text{Zn}_x\text{Fe}_2\text{O}_4$ Synthesized by Powder Metallurgy

Mustafa ARAS<sup>1,2,3</sup>, Mümin ŞAHİN<sup>1\*</sup>, Özcan GÜNDOĞDU<sup>2</sup>

<sup>1</sup>Trakya University, Faculty of Engineering, Department of Mechanical Engineering, Edirne, 22180, Türkiye

<sup>2</sup>Kocaeli University, Faculty of Technology, Department of Biomedical Engineering, Kocaeli, 41380, Türkiye

<sup>3</sup>Tekirdağ Namık Kemal University, Faculty of Çorlu Engineering, Department of Biomedical Engineering, Tekirdağ, 59860, Türkiye

**crossref** <http://dx.doi.org/10.5755/j02.ms.30204>

Received 29 November 2021; accepted 07 March 2022

Powder metallurgy (PM) is a modern manufacturing method that allows high-tech materials, alloys and complex shaped parts to be manufactured with precision and almost without the need for finishing operations such as deburring. PM involves powder production, powder processing, forming operations, pressing and sintering or pressure-assisted hot consolidation. This paper reports results on  $\text{Ni}_{1-x}\text{Zn}_x\text{Fe}_2\text{O}_4$  produced by powder metallurgy at different sintering temperatures.  $\text{Ni}_{1-x}\text{Zn}_x\text{Fe}_2\text{O}_4$  is an interesting functional magnetic material due to its special properties such as stability, very good dielectric properties, electrical resistivity, low dielectric loss, chemical stability, etc. all being important in cutting-edge technology. The use of  $\text{Ni}_{1-x}\text{Zn}_x\text{Fe}_2\text{O}_4$  in diverse fields such as the biomedical field i.e. drug delivery is another vibrant research area. SEM imaging was performed for the structural analysis of the produced bulk sample. EDXRF analyses were performed for elemental composition along with SEM images.

**Keywords:** powder metallurgy, ferrites, microstructure, SEM, EDXRF.

### 1. INTRODUCTION

Powder Metallurgy (PM) is one of the modern manufacturing methods for materials processing of engineered parts involving powder production and processing, forming operations, pressing and sintering or pressure-assisted hot consolidation [1]. PM enables the production of high-tech materials, alloys and intricately shaped parts precisely and without the need for finishing processes such as burrs. This article reports the results related to the production of  $\text{Ni}_{1-x}\text{Zn}_x\text{Fe}_2\text{O}_4$  with PM at different sintering temperatures.  $\text{Ni}_{1-x}\text{Zn}_x\text{Fe}_2\text{O}_4$  is used in various fields such as computer technology, electronic devices, biomedical applications and the automotive industry. This widespread use is due to its special properties such as stability, very good dielectric properties, electrical resistance, low dielectric loss and chemical stability.

PM aims to combine various thermal and mechanical deformation principles on various powders (used as raw material) and transform them into useful engineering pieces. The PM is specially made from high melting point metal powders; offering advantages in the production of complex-shaped parts which are difficult to produce by conventional production methods [1]. The advantage of powder metallurgy is that it provides samples with high enough accuracy and shape of the components which can be crucial in terms of material properties and production stages [2]. The majority of metallic powders, ceramic materials, alloys, composites, and compounds have particle sizes ranging from nanometers to several hundred micrometres; not only

available commercially but also may be produced in labs [1].

A powder preparation process in PM involves various methods such as mechanical methods like milling, machining, shotting and graining. Mechanical alloying methods, chemical production methods such as gas decomposition, thermal decomposition, liquid precipitation, gas precipitation, and solid-solid reaction synthesis are also utilized. Production by electrolysis and atomization methods like gas atomization, water atomization, turbulent atomization and plasma atomization are also in use [3].

The production process with PM consists of three main steps: powder mixing, mold compaction and sintering. In addition, it is suitable for optional pre-preparation processes (such as adding lubricants to the mold) and additional production steps (such as surface polishing, joining, etc.) [4, 5].

The powder as a raw material is homogeneously mixed followed by a pressing process. The pressing process can be done as a separate step or can be combined with sintering as it can be carried out as a pressure-assisted hot consolidation process.

The pressing step has the following basic functions: Obtaining the desired shape of the piece with the aid of a mold. To keep the amount of porosity at the desired level. To provide sufficient strength for the next stage. Ease of obtaining a product with close properties to the final product without the need for further processing steps such as deburring.

In conventional pressing methods, pressure is usually applied in one direction where various mechanical or

\*Corresponding author. Tel.: +90-284-2261217/1410; fax: +90-284-2261225. E-mail address: [mumins@trakya.edu.tr](mailto:mumins@trakya.edu.tr) (M. Şahin)

hydraulic prestige fixed molds are used. After the pressing process, only the physical binding occurs and the pressed samples contain a considerable amount of porosity [5].

The pressing step is continued after the sintering step. Sintering is a technique of obtaining dense materials from compounds consisting of raw materials such as metals, ceramics, etc. by applying heat energy.

The sintering processes occur together with some desired or undesired differentiation in materials. The main differentiation is in the grain boundaries, their size, shapes and their size distribution as well as pore size and pore size distribution. Significant variations also occur not only in chemical composition, crystal structure, strength, elastic modulus, hardness, fracture toughness, electrical and thermal conductivities but also in liquid and gas permeability. In recent years, microwave and pressureless spark plasma sintering has gained importance in the production of materials, in the synthesis of materials and the emphasis has usually been on production processes [5, 6]. The sintering process basically consists of 4 steps: 1. pre-sintering; 2. initial period of sintering; onset of neck creation and contact angle of the grains becoming shallower at this stage; 3. this stage is the middle part of sintering; further progression of necks and pores diffuse through and growing at grain boundaries (GBs); 4. final stage of sintering. The contact GB area between grains progressively increases and densification occurs during sintering at this stage [7].

This paper reports results on the characterisation of nickel ferrites produced through powder metallurgy. EDXRF was used for the elemental composition along with SEM images. Successful application of powder metallurgy in the production of nickel ferrites in a relatively easy way when compared to more complex and involved techniques may be a way forward in the mass production of these samples.

## 2. MATERIAL AND METHODS

PM process is a versatile and effective route for producing components with combinations of various alloying elements. These alloying elements significantly affect metallurgical, mechanical, optical and electrical properties. In addition to alloying elements, the sintering parameters applied are also very effective on the material properties obtained [8]. This paper reports results on the production and microstructural imaging of Nickel Zinc Ferrite (NZF) through powder metallurgy. Ferrite of the type  $\text{NiFe}_2\text{O}_4$  (NF),  $\text{CoFe}_2\text{O}_4$  (CF) and  $\text{MnFe}_2\text{O}_4$  (MF) with the spinel structure are magnetic ceramics. These ferrites are of great importance in the production of magnetic and electronic components.

Ferrites display interesting magnetic and electrical properties depending on processing conditions, sintering temperature and time as well as their chemical composition as such that NF possesses an inverse spinel structure, in which tetrahedral A-sites are occupied by  $\text{Fe}^{3+}$  ions and octahedral B-sites by  $\text{Fe}^{3+}$  and  $\text{Ni}^{2+}$  ions. It shows ferrimagnetism originating from its antiparallel orientation of spins on A- and B- sites. The particle size increases with increasing temperature causing a reduction of the spinel [9]. Harris et al. [10] have given schematic representations and more detailed information for spinel ferrite structures in

their article. It also has properties that are suitable for magnetic applications. In this context, the magnetic properties of the samples of  $\text{Ni}_{1-x}\text{Zn}_x\text{Fe}_2\text{O}_4$  ( $x = 0.15, 0.50$  and  $0.85$ ) obtained by sintering at  $1000\text{ }^\circ\text{C}$  for 1 hour were determined and detailed by Şahin et al. [11] where the characteristic features are also mentioned.

NZF is an all-around magnetic material with interesting magnetic and electrical properties strongly dependent on the purity of ferrite powder, its microstructure, grain boundary and the chemical preparation [12]. The use of NZF based materials in diverse fields such as biomedical field such as in controlled delivery of anticancer drugs is also under investigation [13]. There are also studies in the literature for different stoichiometric ratios of NZF and various ferrite types involving different production techniques besides powder metallurgy. Some of these several methods are conventional ceramic processing method [14], wet chemical method [15], solid state reaction method [16–18], chemical deposition method [19], hydrothermally synthesized [20–22], solid-phase sintering [23], co-precipitation [24, 25], reverse micelle [26], sol-gel combustion [27], a chemical synthesis route called sol-gel combined metallo-organic decomposition method [9], auto-combustion synthesis [28], ball milling [29] and high-energy milling [30]. By considering the characteristics of the products, comparisons can be made between the methods. The main considerations when it comes to production methods are always the low cost and high performance not to mention an environmentally friendly process with minimum waste and minimum energy use.

In this study, the effects of sintering temperature on micro-structural properties of  $\text{Ni}_{1-x}\text{Zn}_x\text{Fe}_2\text{O}_4$  samples by powder metallurgy have been investigated where NiO, ZnO and  $\text{Fe}_2\text{O}_3$  powders with the purity of  $\geq 99.9\%$  were used as raw materials. Powders prepared according to the stoichiometry for;  $x = 0.15$  (Composition 1) and  $x = 0.85$  (Composition 2) mol. Mechanical mixing was used to obtain a homogeneous powder mixture. In the next step, the powder mixtures are pressed in a hydraulic press making the samples ready for the sintering process. Dimensional measurements were taken right after pressing. The samples were sintered for 1 hour at two different constant sintering temperatures, one being  $1000\text{ }^\circ\text{C}$  and the other one being  $1400\text{ }^\circ\text{C}$ . Dimensional measurements were taken again after the sintering processes followed by SEM imaging together with EDXRF for the structural and elemental analysis of the produced bulk samples. The process steps of the experimental studies are given in Table 1.

**Table 1.** Experimental procedure

1 <sup>st</sup> step	
Supply of raw materials	$\geq 99.9\%$ purity NiO, ZnO, $\text{Fe}_2\text{O}_3$ powders
2 <sup>nd</sup> step	
Sample preparation procedure	a) Measurements of weight b) Mechanical mixings c) Pressing d) Sintering
3 <sup>rd</sup> step	
Characterization of sample properties	a) Measurements of size and weight b) EDXRF analysis c) SEM analysis

### 3. RESULTS AND DISCUSSION

#### 3.1. Experimental results

Details of the physical and chemical properties of the samples are given in Table 2 and Table 3. The sample weight was measured with a precision scale and sample dimensions were measured with a digital compass.  $Ni_{1-x}Zn_xFe_2O_4$  samples are coined as composition 1 (C1) ( $x = 0.15$ ) and composition 2 (C2) ( $x = 0.85$ ), according to their compounds for the remainder of this paper. Sample weights were measured with 0.0001 g precision using a balance-precision scale and dimensions were measured with a 0.01 cm precision balance digital compass. Mean values of measurements were taken after repeated measurements before and after sintering. Table 2 shows the weight and volume loss values of the samples. While the weight loss range is between 2.40070–5.02135 % and the volume decrease of the samples is between 9.9620–5.8270 % after pressing and sintering. The volume decrease and weight values at 1000 °C are smaller for C1 compared to C2. However, the volume decrease value at 1400 °C is higher for C1 than C2. In contrast, we see that weight loss is less for C1 than for C2 at 1400 °C.

**Table 2.** Average volume and weight loss after sintering

Comp.	Sintering temperature, °C	Average volume loss after sintering	Average weight loss after sintering
C1	1000	9.9620 %	2.40070 %
	1400	58.8270 %	3.52495 %
C2	1000	28.8059 %	4.79750 %
	1400	54.2387 %	5.02135 %

Brim over of the powders may occur due to the mold and handling prior to sintering. To decrease this overflowing of powders, extreme care should be taken with the mold design so that samples could be kept at the surface with lower adhesion. Handling of measurement devices and use of protective gear such as proper gloves should be considered in order not to cause any contamination. These would prevent unnecessary weight loss and lead to more efficient use of raw materials.

The EDXRF graphical data of the samples are given in Fig. 1–Fig. 4 where Ni, Zn, O, Fe peaks are visible and small unidentified peaks which are usually from impurities in samples also present. EDXRF measurements were taken from three different areas for each sample and results are provided as mean and standard deviation. These impurities might be due to impurities in raw materials and impurities from the experimental conditions. However, the results of the EDXRF confirm that the desired elemental composition values are achieved. The final elemental distribution values (atomic content (%) and weight content (%)) after sintering obtained from EDXRF results for the C1 are given in Table 3. All the composition results are here. SEM images of the composition C1 are given in Fig. 5–Fig. 10. Three different magnification values were selected for the detection of macro and microstructure in SEM imaging. The microstructure of the samples was examined with Philips XL 30 SFEG SEM 1000/10000/50000X magnifications.

The final elemental distribution values (atomic content (%) and weight content (%)) after sintering obtained from

EDXRF results for the C2 are given in Table 4. SEM images of the composition C2 are given Fig. 11–Fig. 16.

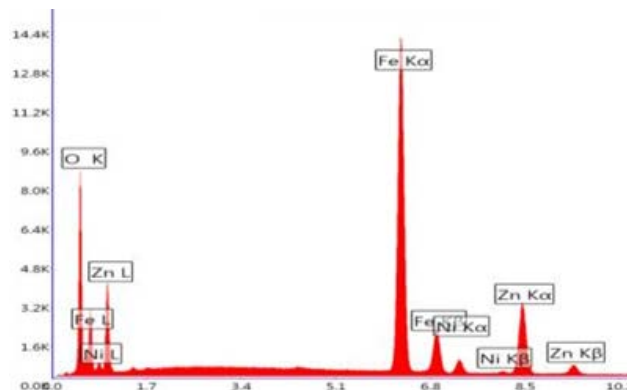


**Fig. 1.** EDXRF analysis of sample C1 – 1000 °C

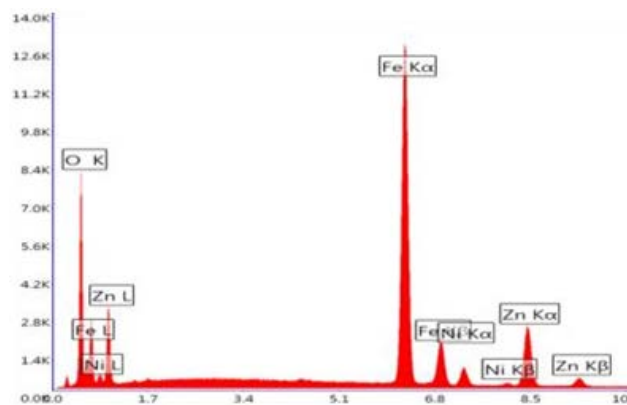


**Fig. 2.** EDXRF analysis of sample C1 – 1400 °C

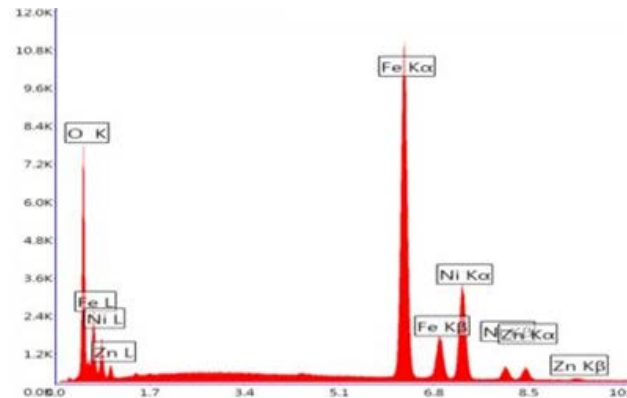


**Fig. 3.** EDXRF analysis of sample C2 – 1000 °C

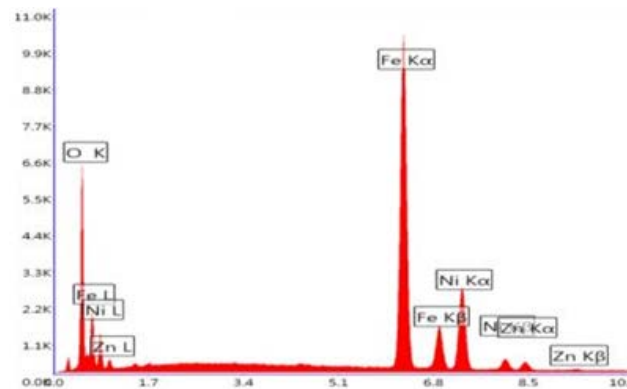


**Fig. 4.** EDXRF analysis of sample C2 – 1400 °C

**Table 3.** Selected samples of C1 content (%) after sintering

C1	Sintering temperature 1000 °C – content, %								Sintering temperature 1400 °C – content, %							
	Ni		Zn		Fe		O		Ni		Zn		Fe		O	
	Mean	SD	Mean	SD	Mean	SD	Mean	SD	Mean	SD	Mean	SD	Mean	SD	Mean	SD
	Atomic content, %								Atomic content, %							
	1.87	0.20	12.29	0.40	30.88	0.74	54.96	0.97	2.24	0.03	10.82	0.03	32.30	0.25	54.64	0.26
	Weight content, %								Weight content, %							
	3.12	0.36	22.84	0.48	49.03	0.59	25.01	0.74	3.74	0.05	20.11	0.11	51.29	0.25	24.86	0.19

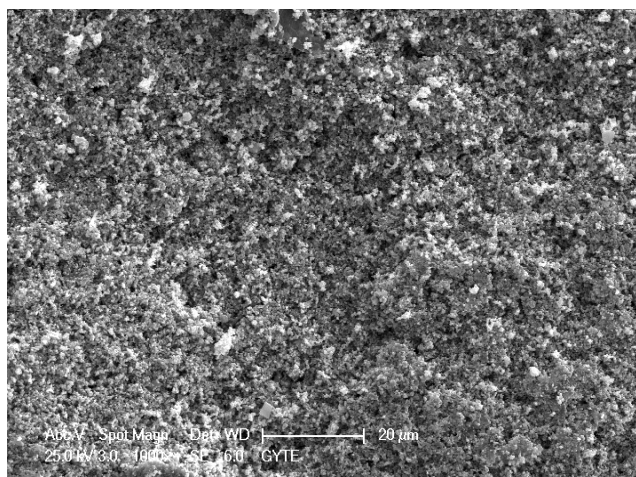


**Fig. 5.** C1 – 1000 °C SEM image of the specimen (1000X)

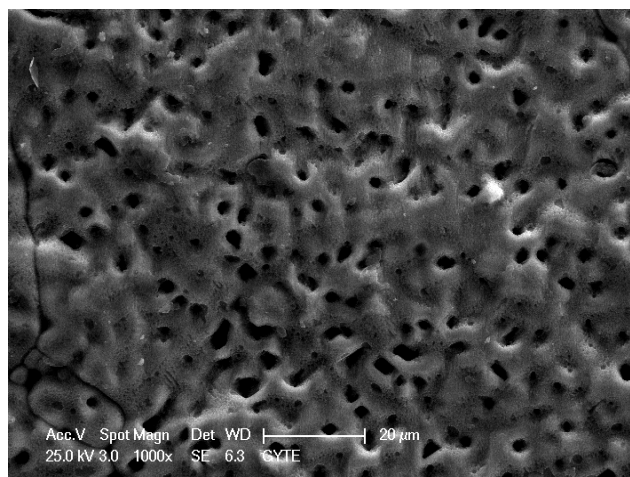


**Fig. 8.** C1 – 1400 °C SEM image of the specimen (1000X)

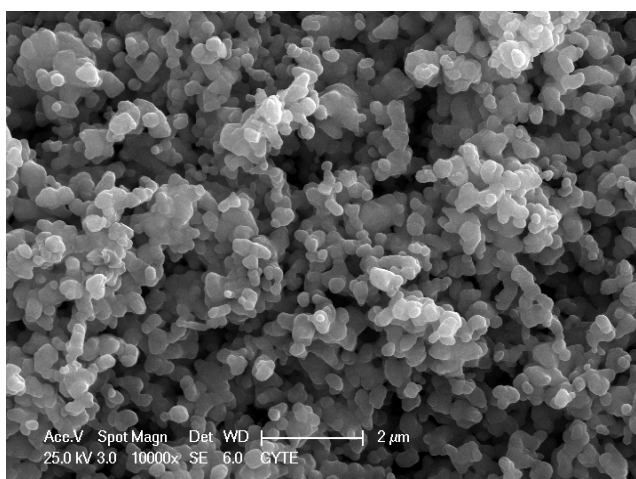


**Fig. 6.** C1 – 1000 °C SEM image of the specimen (10000X)

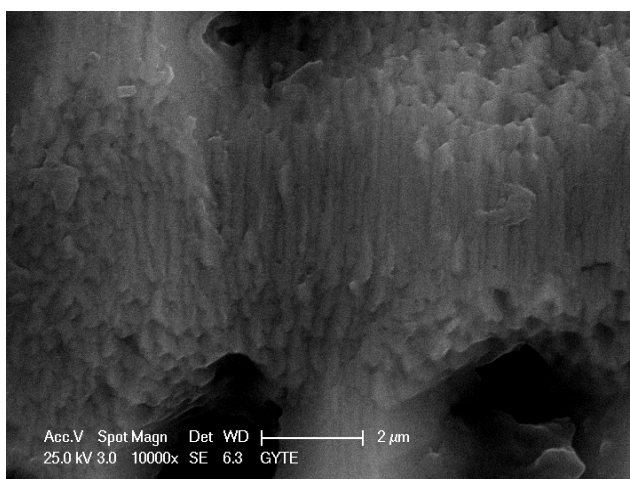


**Fig. 9.** C1 – 1400 °C SEM image of the specimen (10000X)

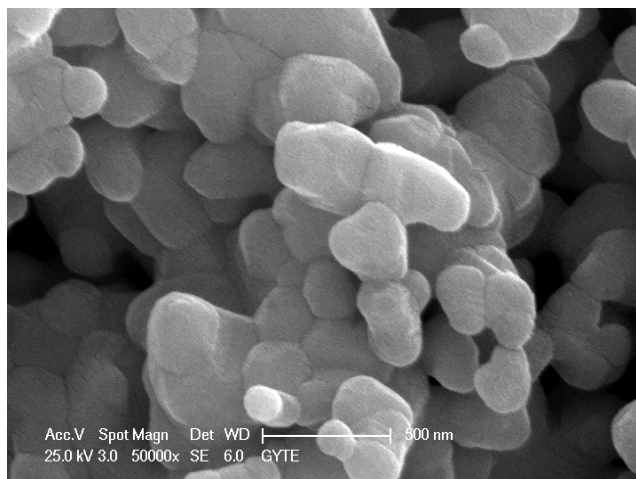


**Fig. 7.** C1 – 1000 °C SEM image of the specimen (50000X)

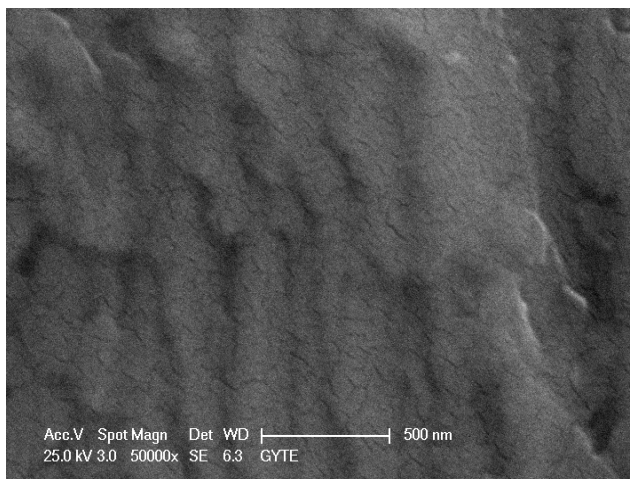


**Fig. 10.** C1 – 1400 °C SEM image of the specimen (50000X)

**Table 4.** Selected samples of C2 content (%) after sintering

C2	Sintering temperature 1000 °C – content, %								Sintering temperature 1400 °C – content, %							
	Ni		Zn		Fe		O		Ni		Zn		Fe		O	
	Mean	SD	Mean	SD	Mean	SD	Mean	SD	Mean	SD	Mean	SD	Mean	SD	Mean	SD
	Atomic content, %								Atomic content, %							
	11.73	0.54	2.05	0.09	30.67	0.26	55.55	0.20	11.54	0.50	1.56	0.03	32.59	0.93	54.31	1.39
Weight content, %								Weight content, %								
20.11	0.87	3.91	0.18	50.03	0.55	25.96	0.16	19.52	0.53	2.95	0.10	52.47	0.65	25.06	1.05	

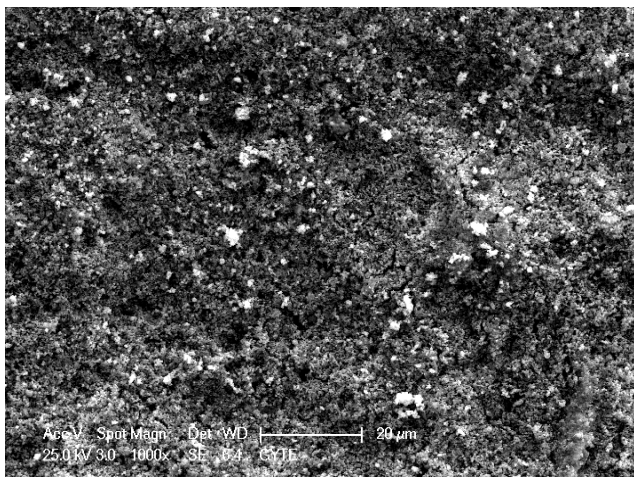


**Fig. 11.** C2 – 1000 °C SEM image of the specimen (1000X)

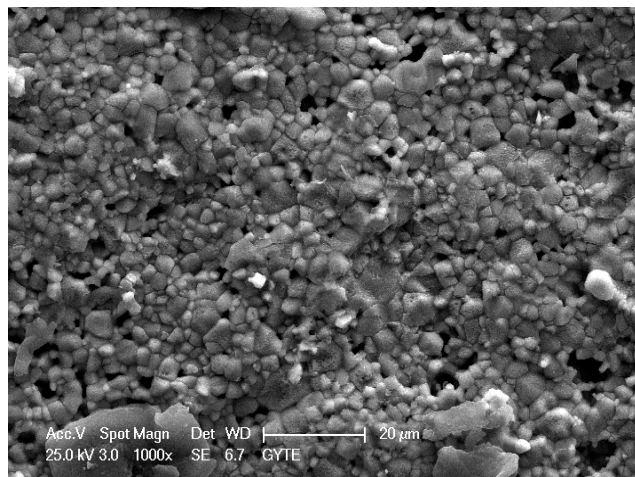


**Fig. 14.** C2 – 1400 °C SEM image of the specimen (1000X)

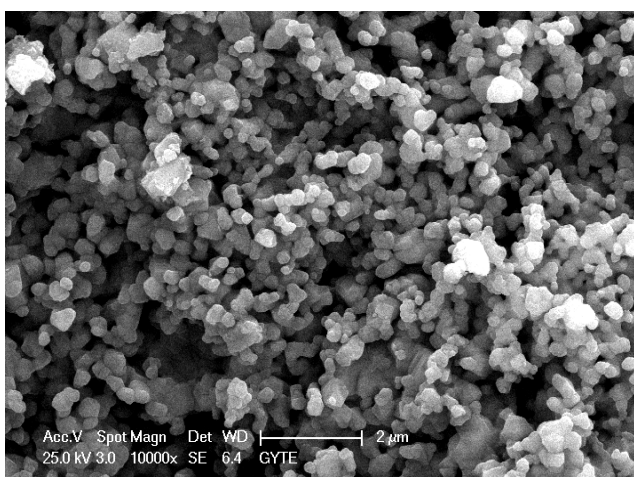


**Fig. 12.** C2 – 1000 °C SEM image of the specimen (10000X)

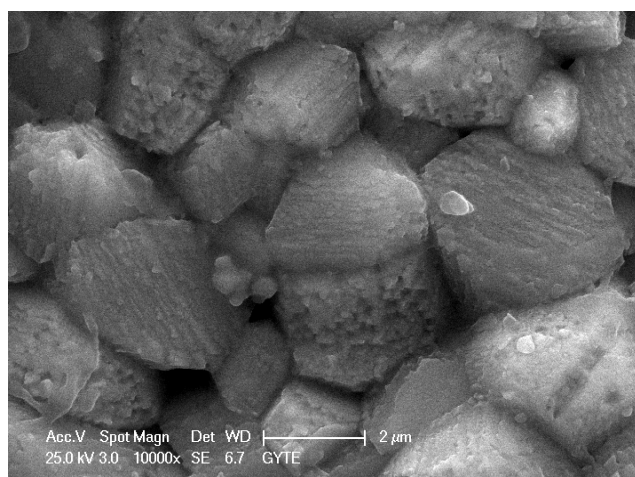


**Fig. 15.** C2 – 1400 °C SEM image of the specimen (10000X)

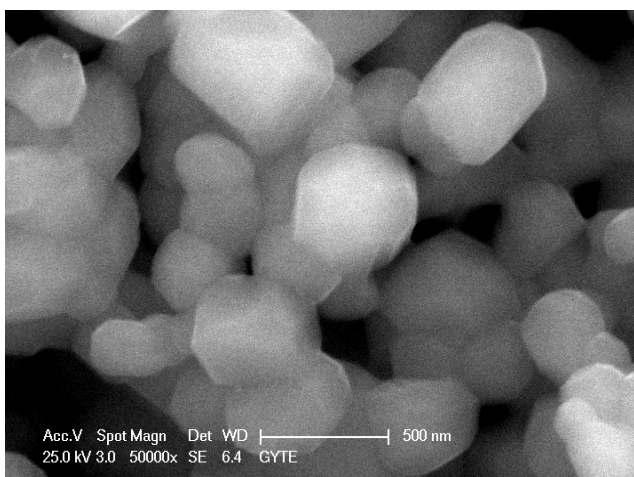


**Fig. 13.** C2 – 1000 °C SEM image of the specimen (50000X)

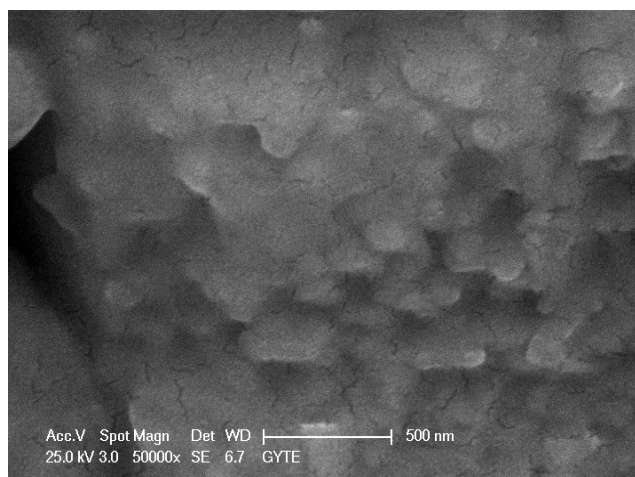


**Fig. 16.** C2 – 1400 °C SEM image of the specimen (50000X)

### 3.2. Discussion

It is well known that the properties of ferrites are strongly influenced by the synthesis conditions, material composition, the impurity levels present, dopants and dopant concentration, microstructure, in the ferrite materials [31]. The data presented above show that the PM method can be used for the production of  $\text{Ni}_{1-x}\text{Zn}_x\text{Fe}_2\text{O}_4$  samples/mass. In our previous publications, the samples were produced with a similar process, but with different production parameters [11, 32, 33] where the main focus was on their magnetic properties. In the current study, the focus is to determine and interpret the effects of low and high sintering temperatures (1000 °C and 1400 °C) on the macro and micro-structural properties of the samples. EDXRF peaks included Fe, Ni, Zn and O. Peak heights depend on the sample content. A comparison can be made with the peaks obtained in the energy dispersive X-ray spectroscopy results obtained in the study of Anupama et al. [31]. Due to the difference in method, compositions and production processes, a one-to-one comparison cannot be expected. However, it can be said that their results support our results presented in this paper. In this study, another experimental step is SEM imaging. 100 to 500 nm grains are seen in SEM images of C1 at 1000 °C as shown in Fig. 5 – Fig. 7 where neck formations have started forming with generally spherical shaped particles. The SEM images of C1 samples after sintering at 1400 °C are given in Fig. 8 – Fig. 10. Yadoji et al. [34] reported in their article that the  $\text{Ni}_{1-x}\text{Zn}_x\text{Fe}_2\text{O}_4$  structure corresponds to crystal structure expansion due to the substitution of larger Zn ions for smaller Ni ions. This is the main reason for the differences between the microstructures of the C1 and C2 compositions in our study. The importance of these materials stems not only from their wide range of applications, but also from different compositional substitutions that lead to improved properties [31]. For this reason, the other composition prepared is C2. The SEM images of the C2 sintered at 1000 °C are shown in Fig. 11 – Fig. 13 are similar to the C1 – 1000 °C images. However, there are differences in average grain sizes when compared to C1 – 1000 °C samples depending on the chemical composition as also evident from the images and EDXRF data. The SEM images of C2 samples after sintering at 1400 °C are given in Fig. 13 – Fig. 16.

It is observed that sintering occurs in C1 samples and pores are closed, whereas in C2 samples, after sintering, grains of more than 2  $\mu\text{m}$  were formed by intergranular intercalations and grain boundaries accompanied by intergranular spaces. The PM method we used to produce samples is not suitable enough for thin-film production. However, there are studies on thin film production to expand the usage areas of  $\text{Ni}_{1-x}\text{Zn}_x\text{Fe}_2\text{O}_4$ . In this context, Gupta et al. [35] produced different compositions with the general combination of  $\text{Ni}_{1-x}\text{Zn}_x\text{Fe}_2\text{O}_4$  with the spin deposition technique. The citrate precursor method was used to prepare the coating solution used for film deposition. With this method, they were able to obtain single-phase, transparent, homogeneous and crack-free nanocrystalline ferrite thin films at low annealing temperatures [35].

It is expected that the volume and weight will decrease as the sintering temperature increases depending on the compounds. This is supported by the experimental results presented herein. However, when a compositional comparison is made, it is observed in Table 2 that as the Zn ratio increases for 1000 °C, the volumetric and weight reduction increases effectively after the sintering. Furthermore, it was determined that as the Zn ratio increased, the weight % decrease was higher for the samples sintered at 1400 °C, but on the other hand, the % wt reduction still remained below the C1 composition in the C2 composition. This is an interesting result that does not agree with the literature. In this study, our focus is the effect of sintering temperature on the microstructure of  $\text{Ni}_{1-x}\text{Zn}_x\text{Fe}_2\text{O}_4$  samples produced by the PM method. Furthermore, the effect of the sintering method such as microwave sintering could be a valuable addition to the literature. Penchal Reddy et al. [36] reported a study using the microwave sintering method where they produced  $\text{Ni}_{1-x}\text{Zn}_x\text{Fe}_2\text{O}_4$  ( $x = 0.2, 0.3, 0.4$  and  $0.5$ ) samples at 900 °C, 1000 °C and 1100 °C sintering temperatures for 30 minutes. Although, a direct comparison is not suitable due to method difference, the main difference between conventional and microwave sintering processes is in the heating mechanism.

Gupta et al. discussed co-precipitation, combustion method, sol-gel process, spray pyrolysis, microemulsion technique, pulsed wire discharge, soft mechanical chemical pathway, chemical vapor deposition and hydrothermal processes for nickel ferrite synthesis. However, powder metallurgy is not mentioned. The powder metallurgy method, which we have successfully applied here, should also take its place among the production methods of nickel ferrites [37].

In addition, Anu and Hemalatha carried out Zn-contributed nickel ferrite particle production studies with co-precipitation technique.  $\text{Zn}_x\text{Ni}_{(1-x)}\text{Fe}_2\text{O}_4$  spherical nanoparticles of different sizes, 15 – 20 nm, 20 – 24 nm and 23 – 30 nm, were obtained in the study. Anu and Hemalatha's working process can be followed if nano-level particles are to be obtained that are smaller than the level shown by the SEM images in our study [38]. Anupama et al. reported the successful synthesis of Ni-Zn nanoparticles by low temperature self-combustion technique. The structural properties of  $\text{Ni}_{1-x}\text{Zn}_x\text{Fe}_2\text{O}_4$  ( $x = 0.0, 0.2, 0.4, 0.6, 0.8$  and  $1.0$ ) were investigated. Alternatively, by careful application of this method, the formation of a single-phase cubic spinel structure without any impurity phases can be achieved as Anupama et al. [39]. Ultimately; there are various chemical and physical production approaches in the literature for the synthesis of nanoferrites. Various methods such as mechanical milling, inert gas condensation, co-precipitation, hydrothermal, sol-gel, sol-gel auto combustion, ultrasonic wave-assisted ball milling, and electro-deposition process have been used for the synthesis of Ni-Zn ferrite. Each process has an impact on one or more of the important properties such as particle size, morphology, catalytic activity, dielectric, and magnetic properties. To compare the results obtained in our study, different techniques can be tried and new data can be obtained [40, 41].

## 4. CONCLUSIONS

Ferrites have gained attention over the past few decades due to their wide range of applications. Increasing interest in different processes to design and produce, especially with respect to low-cost materials with advanced properties continues today and this paper demonstrates that these functional materials can be produced with desired properties in a relatively simple and economical way. In this study, a successful synthesis of  $\text{Ni}_{1-x}\text{Zn}_x\text{Fe}_2\text{O}_4$  ( $x = 0.15$  and  $0.85$ ) using two different sintering temperatures ( $1000^\circ\text{C}$  and  $1400^\circ\text{C}$ ) was reported by the powder metallurgy method. The effect of the sintering temperature on its micro-structural properties has been investigated.

The results indicate that higher concentrations of  $\text{Zn}^{2+}$  can influence both the microstructure and the determination of suitable sintering temperature. Bulk density in all the samples was found to increase with increased sintering temperature. Zn content has different effects on the microstructure. It is safe to assume that  $\text{Ni}_{1-x}\text{Zn}_x\text{Fe}_2\text{O}_4$  with optimum properties can be obtained by the present powder metallurgy process.

The results given here demonstrate that these types of functional materials can be produced with desired parameters and can be considered to be one of the first examples reported in the literature with respect to sintering and chemical composition. The use of powder metallurgy provides a relatively easy and versatile way forward in the production of nickel ferrites as demonstrated herein.

## Acknowledgments

In this study, the experimental data obtained during Mustafa ARAS's Master's Thesis (under the supervision of Prof. Mümin ŞAHİN), was used. The Master's Thesis was supported by Trakya University with the TUBAP-2011/149 project.

The authors would like to thank to İstanbul Technical University, Gebze Technical University, Kocaeli University and Trakya University, Türkiye for their help in the experimental part of the study. The authors would also like to thank Prof Ali GENCER of Ankara University for his useful comments. With respect to Prof. Orhan KAMER of İstanbul Technical University.

## REFERENCES

1. **Kieback, B., Neubrand, A., Riedel, H.** Processing Techniques for Functionally Graded Materials *Materials Science and Engineering: A* 362 (1–2) 2003: pp. 81–106. [https://doi.org/10.1016/s0921-5093\(03\)00578-1](https://doi.org/10.1016/s0921-5093(03)00578-1)
2. **Yamanoğlu, R., Bradbury, W., Karakulak, E., Olevsky, E.A., German, R.M.** Characterisation of Nickel Alloy Powders Processed by Spark Plasma Sintering *Powder Metallurgy* 57 (5) 2014: pp. 380–386. <https://doi.org/10.1179/1743290114y.0000000088>
3. **Angelo, C.P., Subramanian, R.** Powder Metallurgy: Science, Technology and Applications. 2<sup>nd</sup> Printing. New Delhi: PHI Learning Private Limited, ISBN-978-81-203-3281-2, 2009.
4. **Madhukar, P., Selvaraj, N., Rao, C.** Manufacturing of Aluminium Nano Hybrid Composites: A State of Review *IOP Conference Series: Materials Science and Engineering* 149 (012114) 2016: pp. 1–12. <https://doi.org/10.1088/1757-899x/149/1/012114>
5. **Söyler, A.U.** Production of Fe-Mn-Si Based Shape Memory Alloys Via Advanced Powder Metallurgy Techniques *İTÜ Graduate School of Science Engineering and Technology Department of Metallurgy and Materials Engineering PhD Thesis* 2014.
6. **Yamanoğlu, R., Bradbury, W.L., Olevsky, E.A., German, R.M.** Comparative Evaluation of Densification and Grain Size of  $\text{ZnO}$  Powder Compacts During Microwave and Pressureless Spark Plasma Sintering *Advances in Applied Ceramics* 111 (7) 2012: pp. 422–426. <https://doi.org/10.1179/1743676112y.0000000017>
7. **Tanaka, H., Yamamoto, A., Shimoyama, J., Ogino, H., Kishio, K.** Strongly Connected Ex Situ  $\text{MgB}_2$  Polycrystalline Bulks Fabricated by Solid-State Self-Sintering *Superconductor Science and Technology* 25 (11) 2012: pp. 1150221. <https://doi.org/10.1088/0953-2048/25/11/115022>
8. **Erden, M.A., Gündüz, S., Türkmen, M., Karabulut, H.** Microstructural Characterization and Mechanical Properties of Microalloyed Powder Metallurgy Steels *Materials Science and Engineering: A* 616 2014: pp. 201–206. <https://doi.org/10.1016/j.msea.2014.08.026>
9. **Chand Verma, K., Pratap Singh, V., Ram, M., Shah, J., Kotnala, R.K.** Structural, Microstructural and Magnetic Properties of  $\text{NiFe}_2\text{O}_4$ ,  $\text{CoFe}_2\text{O}_4$  and  $\text{MnFe}_2\text{O}_4$  Nanoferrite Thin Films *Journal of Magnetism and Magnetic Materials* 323 (24) 2011: pp. 3271–3275. <https://doi.org/10.1016/j.jmmm.2011.07.029>
10. **Harris, V.G., Geiler, A., Chen, Y., Yoon, S.D., Wu, M., Yang, A., Chen, Z., He, P., Parimi, P.V., Zuo, X., Patton, C.E., Abe, M., Acher, O., Vittoria, C.** Recent Advances in Processing and Applications of Microwave Ferrites *Journal of Magnetism and Magnetic Materials* 321 (14) 2009: pp. 2035–2047. <https://doi.org/10.1016/j.jmmm.2009.01.004>
11. **Sahin, M., Misirli, C., Aras, M.** Characteristic and Magnetic Properties of  $\text{Ni}_{1-x}\text{Zn}_x\text{Fe}_2\text{O}_4$  Ferrites *Waterialwissenschaft und Werkstofftechnik* 47 (1) 2016: pp. 53–63. <https://doi.org/10.1002/mawe.201500464>
12. **Ahmad, A.F., Abbas, Z., Obaiys, S.J., Ibrahim, N.A., Zainuddin, M.F., Salem, A.** Permittivity Properties of Nickel Zinc Ferrite-Oil Palm Empty Fruit Bunch-Polycaprolactone Composite *Procedia Chemistry* 19 2016: pp. 603–610. <https://doi.org/10.1016/j.proche.2016.03.059>
13. **Qasim, M., Asghar, K., Dharmapuri, G., Das, D.** Investigation of Novel Superparamagnetic  $\text{Ni}_{0.5}\text{Zn}_{0.5}\text{Fe}_2\text{O}_4$ @albumen Nanoparticles for Controlled Delivery of Anticancer Drug *Nanotechnology* 28 (36) 2017: pp. 365101–18. <https://doi.org/10.1088/1361-6528/aa7d81>
14. **Zhao, D.L., Lv, Q., Shen, Z.M.** Fabrication and Microwave Absorbing Properties of Ni–Zn Spinel Ferrites *Journal of Alloys and Compounds* 480 (2) 2009: pp. 634–638. <https://doi.org/10.1016/j.jallcom.2009.01.130>
15. **Bhuiyan, M.A., Hoque, S.M., Choudhury, S.** Effects of Sintering Temperature on Microstructure and Magnetic Properties of  $\text{NiFe}_2\text{O}_4$  Prepared from Nano Size Powder of

- NiO and Fe<sub>2</sub>O<sub>3</sub> *Journal of Bangladesh Academy of Sciences* 34 (2) 2011: pp. 189–195.  
<https://doi.org/10.3329/jbas.v34i2.6865>
16. **Adhlakha, N., Yadav, K.L.** Structural, Dielectric, Magnetic, and Optical Properties of Ni<sub>0.75</sub>Zn<sub>0.25</sub>Fe<sub>2</sub>O<sub>4</sub>-BiFeO<sub>3</sub> Composites *Journal of Materials Science* 49 (13) 2014: pp. 4423–4438.  
<https://doi.org/10.1007/s10853-014-8139-x>
  17. **Adhlakha, N., Yadav, K.L.** Study of Dielectric, Magnetic and Magnetoelectric Behavior of (x)NZF-(1-x)PLSZT Multiferroic Composites *IEEE Transactions on Dielectrics and Electrical Insulation* 21 (5) 2014: pp. 2055–2061.  
<https://doi.org/10.1109/tdei.2014.004400>
  18. **Zabotto, F.L., Gualdi, A.J., Eiras, J.A., Oliveira, A.J.A., Garcia, D.** Influence of the Sintering Temperature on the Magnetic and Electric Properties of NiFe<sub>2</sub>O<sub>4</sub> Ferrites *Materials Research* 15 (3) 2012: pp. 428–433.  
<https://doi.org/10.1590/s1516-14392012005000043>
  19. **Pawar, D.K., Shaikh, J.S., Pawar, B.S., Pawar, S.M., Patil, P.S., Kolekar, S.S.** Synthesis of Hydrophilic Nickel Zinc Ferrite Thin Films by Chemical Route for Supercapacitor Application *Journal of Porous Materials* 19 (5) 2011: pp. 649–655.  
<https://doi.org/10.1007/s10934-011-9516-3>
  20. **Datt, G., Abhyankar, A.C.** Structural, Magnetic and Dielectric Properties of NiZnFe<sub>2</sub>O<sub>4</sub> Nanocrystals *AIP Conference Proceedings* 1724 2016: pp. 020039.  
<https://doi.org/10.1063/1.4945159>
  21. **Singh, S., Singh, M., Kotnala, R.K., Verma, K.C.** Hydrothermal Synthesis of NiFe<sub>2</sub>O<sub>4</sub>, Ni<sub>0.6</sub>Zn<sub>0.4</sub>Fe<sub>2</sub>O<sub>4</sub> and Ni<sub>0.6</sub>Zn<sub>0.4</sub>Fe<sub>2</sub>O<sub>4</sub>/SrFe<sub>2</sub>O<sub>4</sub>: Nanostructure, Magnetic and Dielectric Properties *Indian Journal of Pure & Applied Physics* 52 2014: pp. 550–555.
  22. **Chandra Babu Naidu, K., Madhuri, W.** Hydrothermal Synthesis of NiFe<sub>2</sub>O<sub>4</sub> Nano-Particles: Structural, Morphological, Optical, Electrical and Magnetic Properties *Bulletin of Materials Science* 40 (2) 2017: pp. 417–425.  
<https://doi.org/10.1007/s12034-017-1374-4>
  23. **Niemiec, P., Bochenek, D., Chrobak, A., Guzdek, P., Blachowski, A.** Ferroelectric-Ferromagnetic Ceramic Composites Based on PZT with Added Ferrite *International Journal of Applied Ceramic Technology* 12 2014: pp. E82–E89.  
<https://doi.org/10.1111/ijac.12260>
  24. **Gul, I.H., Ahmed, W., Maqsood, A.** Electrical and Magnetic Characterization of Nanocrystalline Ni–Zn Ferrite Synthesis by Co-Precipitation Route *Journal of Magnetism and Magnetic Materials* 320 (3–4) 2008: pp. 270–275.  
<https://doi.org/10.1016/j.jmmm.2007.05.032>
  25. **Shahane, G.S., Kumar, A., Arora, M., Pant, R.P., Lal, K.** Synthesis and Characterization of Ni–Zn Ferrite Nanoparticles *Journal of Magnetism and Magnetic Materials* 322 (8) 2010: pp. 1015–1019.  
<https://doi.org/10.1016/j.jmmm.2009.12.006>
  26. **Thakur, S., Katyal, S.C., Singh, M.** Structural and Magnetic Properties of Nano Nickel–Zinc Ferrite Synthesized by Reverse Micelle Technique *Journal of Magnetism and Magnetic Materials* 321 (1) 2009: pp. 1–7.  
<https://doi.org/10.1016/j.jmmm.2008.07.009>
  27. **Azadmanjiri, J.** Structural and Electromagnetic Properties of Ni–Zn Ferrites Prepared by Sol-Gel Combustion Method *Materials Chemistry and Physics* 109 (1) 2008: pp. 109–112.  
<https://doi.org/10.1016/j.matchemphys.2007.11.001>
  28. **Deka, S., Joy, P.A.** Characterization of Nanosized NiZn Ferrite Powders Synthesized by an Autocombustion Method *Materials Chemistry and Physics* 100 (1) 2006: pp. 98–101.  
<https://doi.org/10.1016/j.matchemphys.2005.12.012>
  29. **Gheisari, K., Shahriari, S., Rezvanpour, A., Javadpour, S.** Structure and Magnetic Properties of Nanocrystalline Ni<sub>0.64</sub>Zn<sub>0.36</sub>Fe<sub>2</sub>O<sub>4</sub> Powders Prepared by Ball Milling *Powder Metallurgy* 56 (3) 2013: pp. 216–220.  
<https://doi.org/10.1179/1743290113y.0000000051>
  30. **Yu, L., Zhang, J., Liu, Y., Jing, C., Cao, S.** Fabrication, Structure and Magnetic Properties of Nanocrystalline NiZn-Ferrite by High-Energy Milling *Journal of Magnetism and Magnetic Materials* 288 2005: pp. 54–59.  
<https://doi.org/10.1016/j.jmmm.2004.08.024>
  31. **Anupama, M.K., Srinatha, N., Matteppanavar, S., Angadi, B., Sahoo, B., Rudraswamy, B.** Effect of Zn Substitution on the Structural and Magnetic Properties of Nanocrystalline NiFe<sub>2</sub>O<sub>4</sub> Ferrites *Ceramics International* 44 (5) 2018: pp. 4946–4954.  
<https://doi.org/10.1016/j.ceramint.2017.12.087>
  32. **Sahin, M., Misirli, C., Aras, M.** On Production of Magnetic Materials Having Ni<sub>1-x</sub>Zn<sub>x</sub>Fe<sub>2</sub>O<sub>4</sub> *Proceedings of the Second International Conference on Advances in Mechanical and Robotics Engineering-AMRE 2014* 2014: pp. 24–28.  
<https://doi.org/10.15224/978-1-63248-031-6-144>
  33. **Aras, M., Sahin, M.** Ni<sub>0.15</sub>Zn<sub>0.85</sub>Fe<sub>2</sub>O<sub>4</sub> Numunelerin Toz Metalurjisi Yöntemiyle Üretimi ve 1200 °C Sinterleme Sonrası Mikroyapısal İncelenmesi *2<sup>nd</sup> International Congress on Engineering Architecture and Design* 2017: pp. 775–776.
  34. **Yadoji, P., Peelamedu, R., Agrawal, D., Roy, R.** Microwave Sintering of Ni-Zn Ferrites: Comparison with Conventional Sintering *Materials Science and Engineering: B* 98 (3) 2003: pp. 269–278.  
[https://doi.org/10.1016/s0921-5107\(03\)00063-1](https://doi.org/10.1016/s0921-5107(03)00063-1)
  35. **Gupta, N., Verma, A., Kashyap, S.C., Dube, D.C.** Microstructural, Dielectric and Magnetic Behavior of Spin-Deposited Nanocrystalline Nickel-Zinc Ferrite Thin Films for Microwave Applications *Journal of Magnetism and Magnetic Materials* 308 (1) 2007: pp. 137–142.  
<https://doi.org/10.1016/j.jmmm.2006.05.015>
  36. **Reddy, M.P., Madhuri, W., Reddy, N.R., Kumar, K.V.S., Murthy, V.R.K., Reddy, R.R.** Magnetic Properties of Ni-Zn Ferrites Prepared by Microwave Sintering Method *Journal of Electroceramics* 28 (1) 2011: pp. 1–9.  
<https://doi.org/10.1007/s10832-011-9670-7>
  37. **Gupta, N., Jain, P., Rana, R., Shrivastava, S.** Current Development in Synthesis and Characterization of Nickel Ferrite Nanoparticle *Materials Today: Proceedings* 4 (2) 2017: pp. 342–349.  
<https://doi.org/10.1016/j.matpr.2017.01.031>
  38. **Anu, K., Hemalatha, J.** Synthesis and Analysis of Structural, Compositional, Morphological, Magnetic, Electrical and Surface Charge Properties of Zn-Doped Nickel Ferrite Nanoparticles *Ceramics International* 48 (3) 2022: pp. 3417–3425.  
<https://doi.org/10.1016/j.ceramint.2021.10.118>
  39. **Anupama, M.K., Rudraswamy, B., Dhananjaya, N.** Investigation on Impedance Response and Dielectric Relaxation of Ni-Zn Ferrites Prepared by Self-Combustion Technique *Journal of Alloys and Compounds* 706 2017: pp. 554–561.  
<https://doi.org/10.1016/j.jallcom.2017.02.241>

40. **Rahimi, M., Kameli, P., Ranjbar, M., Hajihashemi, H., Salamati, H.** The Effect of Zinc Doping on the Structural and Magnetic Properties of  $\text{Ni}_{1-x}\text{Zn}_x\text{Fe}_2\text{O}_4$  *Journal of Materials Science* 48 (7) 2013: pp. 2969 – 2976.  
<https://doi.org/10.1007/s10853-012-7074-y>
41. **Aafiya Abushad, M., Arshad, M., Naseem, S., Ahmed, H., Ansari, A., Chakradhary, V.K., Husain, S., Khan, W.**

Synthesis and Role of Structural Disorder on the Optical, Magnetic and Dielectric Properties of Zn Doped  $\text{NiFe}_2\text{O}_4$  Nanoferrites *Journal of Molecular Structure* 1253 2022: pp. 132205 1 – 16.  
<https://doi.org/10.1016/j.molstruc.2021.132205>



© Aras et al. 2022 Open Access This article is distributed under the terms of the Creative Commons Attribution 4.0 International License (<http://creativecommons.org/licenses/by/4.0/>), which permits unrestricted use, distribution, and reproduction in any medium, provided you give appropriate credit to the original author(s) and the source, provide a link to the Creative Commons license, and indicate if changes were made.